GREEN SYNTHESIS OF CRYSTALLINE STRONTIUM NITRATE NANOPARTICLES USING THYME EXTRACT AND THEIR APPLICATION IN A POTENTIOMETRIC PROCAINE SENSOR

M.M. Abdullah*, K.S. Hussein

Kirkuk University, College of Science, Department of Chemistry, Kirkuk, Iraq.
**e-mail: marwahmahmood@uokirkuk.edu.iq*

Received 11.01.2026
Accepted 06.04.2026

***Abstract**: This work presents the development of a novel potentiometric sensor for the accurate and selective quantification of procaine. The primary sensing element employs crystalline strontium nitrate nanoparticles (SrNPs) synthesized via an environmentally friendly and sustainable method, whereby an aqueous extract of Thymus vulgaris serves as both a bioreducing agent and a capping agent. The nanoparticles were characterized by UV-Vis spectroscopy, FT-IR, X-ray diffraction (XRD), and scanning electron microscopy (SEM). The results confirmed the formation of crystalline strontium-based nanoparticles with an average crystallite size of 29 nm and irregular morphology. These nanoparticles were then incorporated into a modified carbon electrode containing a polyvinyl chloride (PVC) matrix and a procaine-phosphomolybdic acid (PCA-PMA) ion-pair complex as the sensing component. The sensor exhibited a wide linear response range from 1.0 × 10^{-2} M to 1.0 × 10^{-7} M, a near-Nernstian slope of 22.8 mV per decade, and a low detection limit of 6.8 × 10^{-9} M. The sensor was successfully applied to quantify procaine in commercial pharmaceutical tablets with high accuracy and precision, thus underscoring its potential applicability in drug analysis and quality assurance.*

***Keywords:** Procaine, Potentiometric sensor, Green synthesis, Strontium nanoparticles*

Introduction

Procaine (PCA) is a local anesthetic drug of the amino ester group that acts by blocking voltage-gated sodium channels in neuronal membranes, thereby preventing the generation and conduction of nerve impulses [1]. Clinically, it is mainly used to induce local anesthesia for minor surgical and dental procedures. PCA has also been used in some formulations for managing certain cardiac arrhythmias due to its membrane-stabilizing properties [2, 3]. Chemically, procaine is identified as 2-(diethylamino)ethyl4-aminobenzoate with the molecular-formula $C_{13}H_{20}N_2O_2$. It commonly appears as a white crystalline powder or colorless crystals. Procaine hydrochloride, its water-soluble salt used in injections. The compound exhibits high solubility in aqueous media and shows limited dissolution in alcoholic solvents. The molecular structure of PCA is shown in Fig. 1 [4].

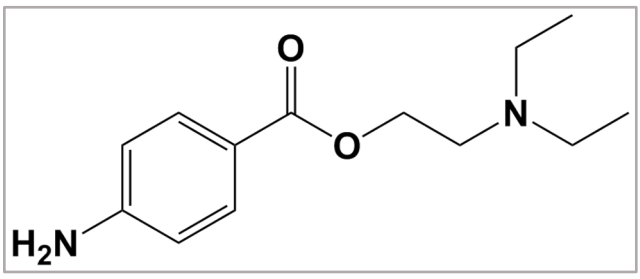

Fig. 1. The structure of PCA [4]

Potentiometric ion-selective electrodes (ISEs) offer important advantages such as ease of use, short response time, wide concentration range, low cost, and good selectivity [5–10]. They are applied in pharmaceutical, food, and environmental analysis [11, 12]. The ionophore is the key component that determines the electrode's selectivity toward the target analyte [13]. Green synthesis of nanoparticles has emerged as a key alternative to traditional methods that often require harsh

chemicals, high energy input, and produce toxic byproducts, raising environmental and safety concerns [14-17]. Green synthesis uses natural, biocompatible, and sustainable materials such as plant extracts that serve as reducing and stabilizing agents [18]. This method can produce nanoparticles with special and improved properties while reducing environmental impact. Strontium-based nanoparticles (SrNPs), in particular, have gained attention for applications in catalysis, bioimaging, and chemical sensing, owing to their distinct physical and chemical characteristics [19].

The current work addresses a need in pharmaceutical analysis by developing a novel potentiometric sensor for the local anesthetic procaine. The main advancement is the use of crystalline strontium nitrate nanoparticles (SrNPs) synthesized via an environmentally friendly method using thyme (Thymus vulgaris) extract as a key component of the sensor membrane. The choice of a botanical extract is not merely ecological; it is scientific approach that takes advantage of the plant's specific phytochemicals. As shown by the FT-IR analysis, thyme extract is rich in bioactive compounds such as phenols (e.g., thymol, carvacrol), which play a crucial role in the reduction of strontium ions and the subsequent stabilization of the nanoparticles [20, 21]. This establishes a direct link between the biological origin and the physical characteristics of the nanoparticles, moving beyond a simple "green" claim to a well-demonstrated scientific procedure.

Experimental part

Apparatus and equipment. Potentiometric measurements were made with a digital pH/millivolt meter (Jenway 3310, China). A saturated calomel electrode (SCE, Me-SC90, England) was used as reference electrode. Weighing was done with a sensitive balance (Sartorius BL210 SAG, Germany). Heating was carried out using a heater (HPL-248, China) and an oven (KARL KOLB, Germany). A magnetic stirrer with a hot plate (Jenway, Germany) was used for mixing and heating solutions. Ultrasonic cleaning was performed with an ultrasonic bath (KARL KOLB, Germany). A UV-Visible double-beam spectrophotometer (T92+, China), an FT-IR spectrometer, an X-ray diffractometer (XRD), and a scanning electron microscope (SEM) were used to analyze the generated nanoparticles.

Reagents and chemical materials. Procaine (PCA) pure standard powder (98%) was supplied by SDI, Iraq. Phosphomolybdic acid (PMA, 98%), Tributyl phosphate (TBP, 99%), Polyvinyl chloride (PVC), Tetrahydrofuran (THF, 99%), and other chemical reagents were obtained from Fluka and BDH. Deionized water was used throughout the experiments for the preparation of all solutions. The following solutions were used in the study: A 1×10^{-1}M hydrochloric acid solution, 1×10^{-1}M sodium hydroxide solution, standard phosphomolybdic acid (PMA) solution (1×10^{-2} M), strontium nitrate solution (1×10^{-1} M), and stock solutions (1×10^{-1}M) of potential interferents including NaCl, KCl, $NaNO_2$, $MnSO_4$, sucrose, and starch were also prepared.

Preparation of solutions.

Standard procaine (PCA) solution (1×10^{-2} M). A primary stock solution of PCA at a concentration of 1.0×10^{-2} M was prepared by accurately weighing 2.91 g of procaine hydrochloride and dissolving it in deionized water. The solution was transferred to a 100 mL volumetric flask and diluted to the mark with deionized water. From this stock, a series of working standard solutions ranging from 1.0×10^{-2} M to 1.0×10^{-7} M were prepared by serial dilution with deionized water.

Sample solution of procaine from tablet (1×10^{-2} -1×10^{-7}M). An accurately weighed amount of mixed powder from three vials of Acacaine injections (each containing 600 mg of procaine penicillin, Acay Production), equivalent to approximately 0.241 g of procaine, was transferred to a 100 mL flask. The powder was dissolved in deionized water, and the volume was adjusted to the mark to obtain a stock solution. From this stock, 11.3 mL was pipetted into a separate 100 mL volumetric flask and diluted to volume with deionized water to give a 0.01 M working standard. A concentration series from 10^{-2} M to 10^{-7} M was then prepared by serial dilution of this working standard.

Thyme Extract. 10.0 g of dried *Thymus vulgaris* leaves were ground using a nanoscale grinder. To extract the bioactive compounds, the powdered leaves were mixed with 150 mL of distilled water

and heated at 80 °C for thirty min. After cooling to 25 °C, the mixture was filtered through filter paper to remove suspended particles. The resulting light brown thyme extract was collected in a conical flask and stored under suitable conditions for later use in nanoparticle synthesis.

Green synthesis of strontium nanoparticles using thyme extract. Strontium nanoparticles (SrNPs) were synthesized using an eco-friendly method. A 0.1 M strontium nitrate solution (50 mL) was heated to 60 °C under constant magnetic stirring. Then, 50 mL of 10% w/v aqueous thyme extract was added dropwise. The pH was adjusted to approximately 10 with 0.1 M NaOH. The mixture was kept in the dark at room temperature for 24 h to allow nanoparticle formation. The precipitate was filtered, washed repeatedly with distilled water and finally with absolute ethanol, and then dried at 80 °C for 24 h. The dried product was calcined in a muffle furnace at 600 °C for 3 h to obtain crystalline SrNPs (Fig. 2).

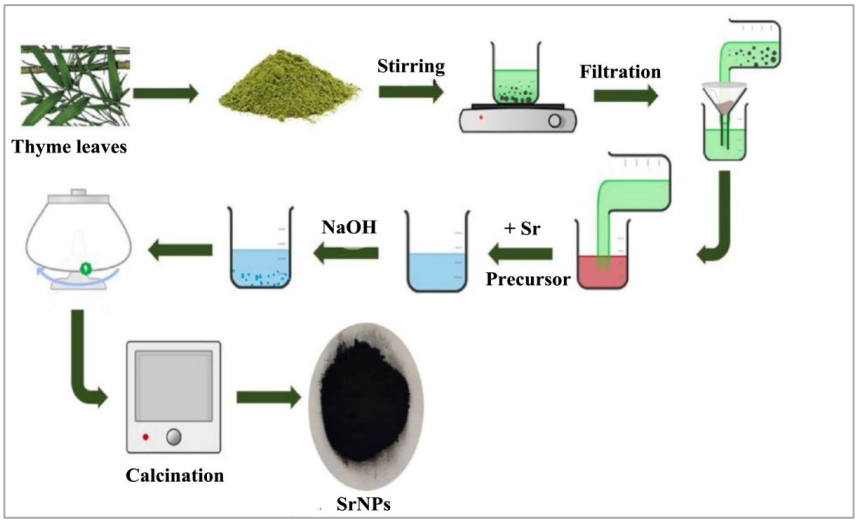

Fig. 2. Synthesis of Strontium nanoparticles

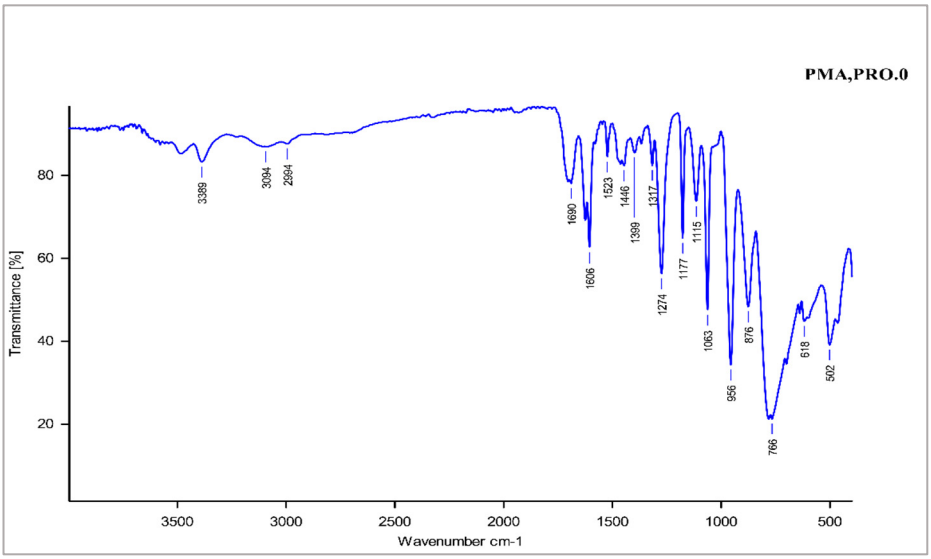

Fig. 3. FT-IR spectrum of ion pair PCA-PMA

Preparation of PCA-PMA ion-pair complex. The PCA-PMA ion-pair complex was synthesized by mixing equimolar aqueous solutions of procaine hydrochloride and phosphomolybdic acid, each at a concentration of 1.0×10^{-2} M, in a total volume of 100 milliliters. A solid product formed immediately. The precipitate was collected by filtration, washed thoroughly with deionized water, and then air-dried at 25 °C for 24 h. The formation of the complex was confirmed by FT-IR spectroscopy. The spectrum (Fig. 3) shows characteristic absorption bands indicating interaction between the ions, confirming successful synthesis.

Fabrication of the coated carbon sensor. A graphite rod (5 cm length, 5 mm diameter) was first cleaned ultrasonically with acetone and deionized water for 10 min to remove any surface contaminants. One end of the rod was inserted into a PVC tube, leaving the other end exposed for electrical connection. The coating solution was prepared by dissolving 0.2 g of PVC, 0.2 mL of tributyl phosphate (TBP) plasticizer, 12 mg of the PCA-PMA ion-pair complex, and 0.006 g of the synthesized SrNPs in 5 mL of tetrahydrofuran (THF). The mixture was stirred until complete dissolution. The exposed tip of the graphite rod was dip-coated by immersing it vertically into the coating solution for 10 s, and then slowly withdrawing it. The solvent was allowed to evaporate at room temperature for 15 min. This dipping-drying cycle was repeated five times to obtain a uniform and adherent membrane layer. The fabricated electrode was conditioned by soaking in a 1.0×10^{-3} M PCA solution for 12 h before use (Fig. 4).

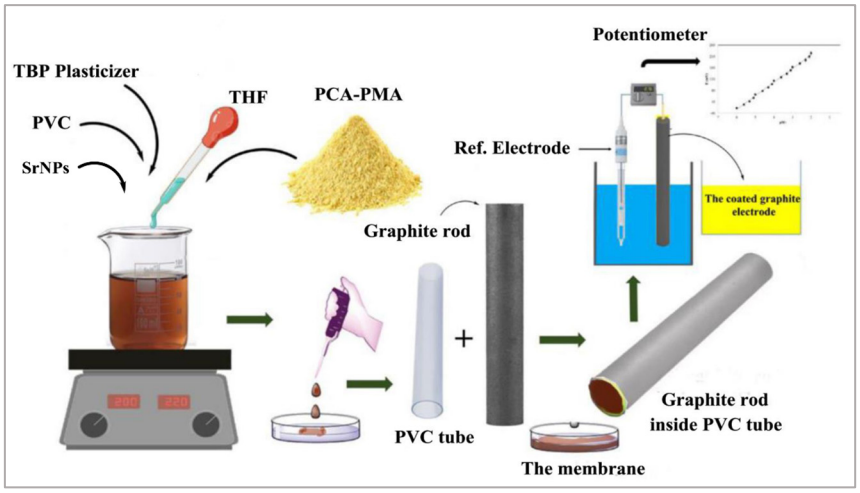

Fig. 4. Fabrication of the coated carbon sensor

Results and discussion

Characterization of strontium nanoparticles.

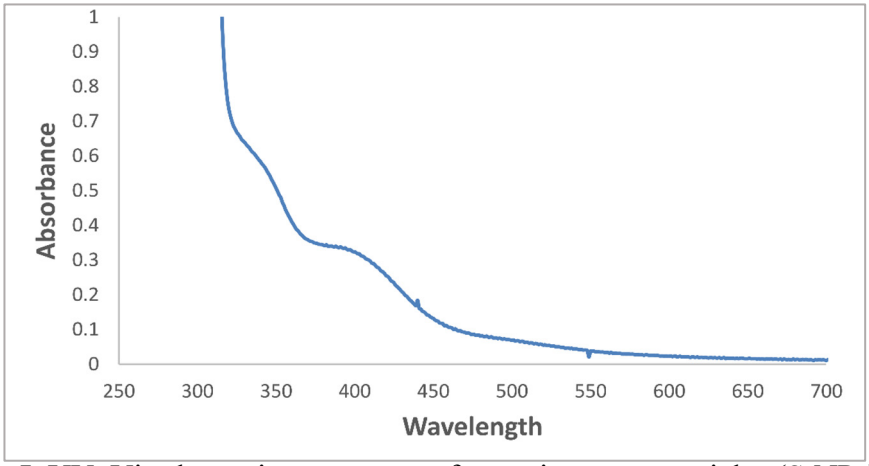

Fig. 5. UV–Vis absorption spectrum of strontium nanoparticles (SrNPs)

UV-Vis spectrum of SrNPs. UV-Vis spectroscopy was used to examine the optical properties of SrNPs in the wavelength range 200-900 nm. Immediately after reduction of strontium ions, a rapid color change was observed, indicating nanoparticle formation. The absorption spectrum (Fig. 5) showed a characteristic peak at $\lambda = 420$ nm. This confirms the formation of stable nanoparticles, which typically absorb in the 380-460 nm range.

FT-IR spectrum of SrNPs. FT-IR analysis was performed to identify the biomolecules in thyme extract responsible for the reduction and stabilization of strontium nanoparticles. A broad hydroxyl stretching band at 3200-3400 cm^{-1} was observed in the spectrum (Fig. 6), attributed to phenolic groups such as carvacrol and thymol. Aliphatic C–H stretching vibrations were identified by peaks at 2920 and 2850 cm^{-1}, whereas aromatic C=C stretching was indicated by the band at 1605 cm^{-1}. Additionally, a C–O stretching band was observed between 1030 and 1220 cm^{-1}, characteristic of phenolic compounds, along with a weak C–N stretching band. These functional groups were involved in both the stabilization of the resultant NPs and the reduction of Sr^{2+} ions.

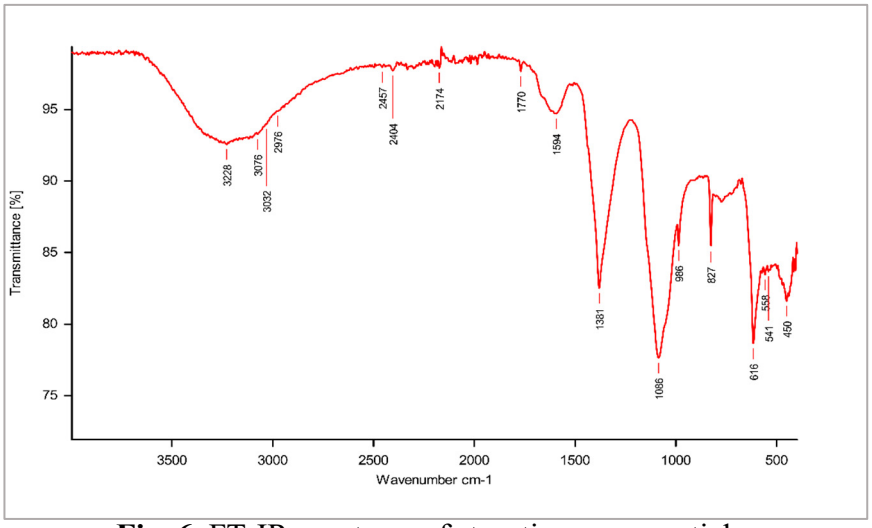

Fig. 6. FT-IR spectrum of strontium nanoparticles

XRD analysis of SrNPs. XRD was performed to confirm the crystalline nature of the nanoparticles synthesized using thyme extract. Fig. 7 shows sharp and intense peaks, indicating the formation of highly crystalline strontium nanoparticles. The calculated crystallite sizes ranged from 14 to 98 nm, with an average of 29 nm (Table 1). These results demonstrate that the bioactive components in the thyme extract acted as reducing and stabilizing agents, effectively controlling nanoparticle growth and ensuring the formation of stable, well-ordered crystalline structures.

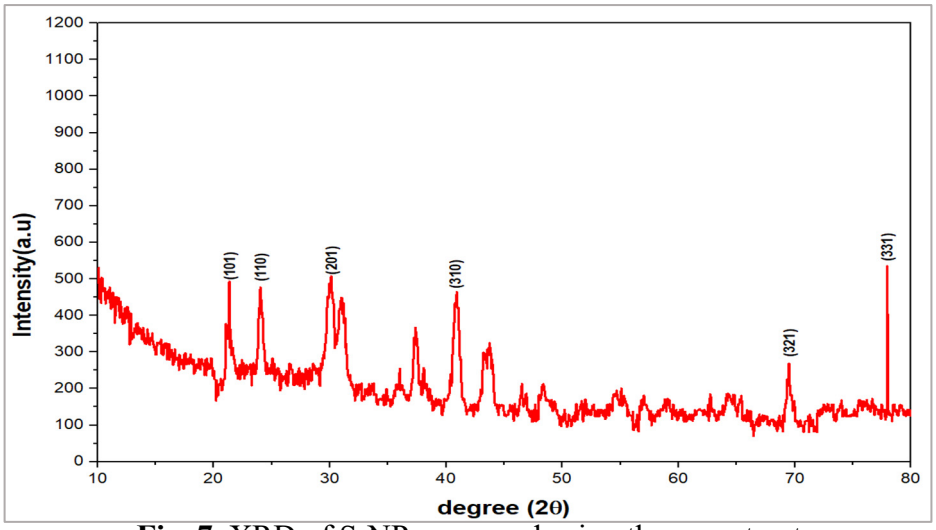

Fig. 7. XRD of SrNPs prepared using thyme extract

Table 1. Crystallite size calculation of SrNPs using the Debye–Scherrer equation

2θ (°)	θ (radians)	FWHM (radians)	cos θ	Crystallite Size D (nm)	Average D (nm)
10.6272	0.18548	0.00687	0.982848	21	29
12.0213	0.209812	0.00687	0.97807	22	

15.0622	0.262886	0.008587	0.965644	17	
15.5727	0.271795	0.010304	0.963291	14	
16.8351	0.293826	0.001571	0.957143	98	
18.0114	0.314334	0.008076	0.951003	19	
18.6872	0.32615	0.00687	0.947283	22	

SEM analysis of SrNPs. The surface structure and morphology of the synthesized SrNPs were examined by SEM. The micrographs (Fig. 8) showed particles with sizes ranging from 35.5 to 85.2 nm and non-uniform morphology. The surfaces exhibited nanoscale folds and protrusions between 12.3 and 42.6 nm. These morphological features enhance surface reactivity and absorptivity, which increase as particle size decreases. These structural characteristics highlight the potential of thyme-mediated SrNPs for advanced applications in biomedicine, sensing, and catalysis.

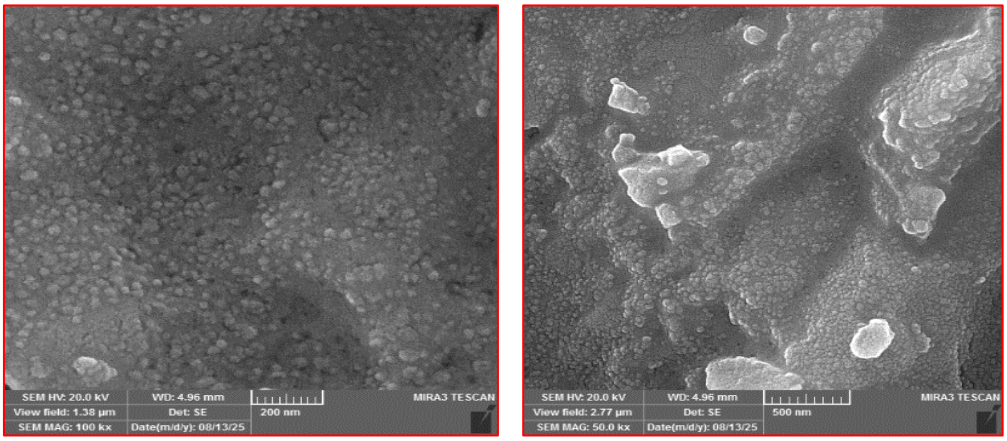

Fig. 8. SEM image of strontium nanoparticles prepared using thyme extract

Role of strontium nanoparticles in sensor performance. Incorporating crystalline SrNPs into the sensor membrane significantly enhances the analytical performance. The high surface area and crystalline nature (confirmed by XRD and SEM) provide additional active sites for the immobilization of the PCA-PMA ion-pair, increasing the effective concentration of the sensing element at the membrane surface. Moreover, the SrNPs facilitate charge transfer between the ion-pair and the graphite support, improving electronic conductivity and reducing the response time. The phenolic functional groups originating from the thyme extract (detected by FT-IR) remain partly associated with the nanoparticle surface, contributing to selective interaction with procaine molecules. This synergy results in the observed near-Nernstian response, wide linear range, and low detection limit.

Study the optimal conditions for the method. After fabricating the nanocoated electrode on the graphite rod and immersing it in a 1×10^{-3} M drug solution for a specific time, the characteristics and specifications of the fabricated nanoelectrode were studied. This included examining the effect of pH, temperature, response time, concentration range, slope, and correlation coefficient, as well as the electrode's lifetime, accuracy, reproducibility, detection limit, selectivity, and applications, all evaluated through potential measurements expressed in mV.

Response time of electrode. The sensor's response time varied with concentration. It was shorter for higher concentrtions (1×10^{-2} M and 1×10^{-3} M), and became progressively longer for more dilute solutions (1×10^{-4} M to 1×10^{-7} M). This trend indicates that reaching equilibrium at the membrane surface is a slower process in dilute solutions than in concentrated ones. The response time depends on several factors, including temperature, viscosity, and the scan rate. The results are shown in Table 2.

Table 2. Electrode's response time.

Sensor	Conc. (M)	Response time (sec)

The nano graphite electrode	1×10^{-2}	7
	1×10^{-3}	10
	1×10^{-4}	14
	1×10^{-5}	19
	1×10^{-6}	25
	1×10^{-7}	33

Impact of pH. Two drug solutions (1×10^{-2} M and 1×10^{-4} M) were tested. Their pH was adjusted using diluted HCl or NaOH over the range pH 2.0-7.0 (Fig. 9). Outside this range, the response became unreliable. Below pH 2.0, increasing acidity enhanced the electrode signal, probably because the membrane itself began to extract hydrogen ions. Above pH 7.0, a decrease in potential was observed. attributed to the deprotonation of the membrane's secondary amino group, which reduces its effective concentration at the surface.

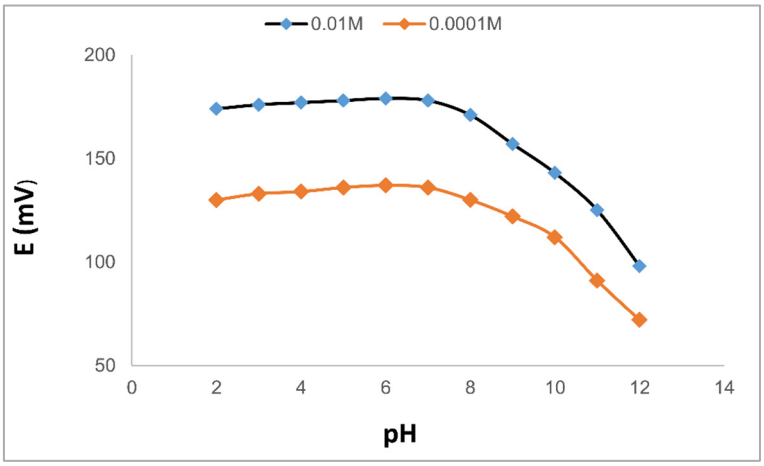

Fig. 9. Impact of pH on the responses of nano graphite electrode.

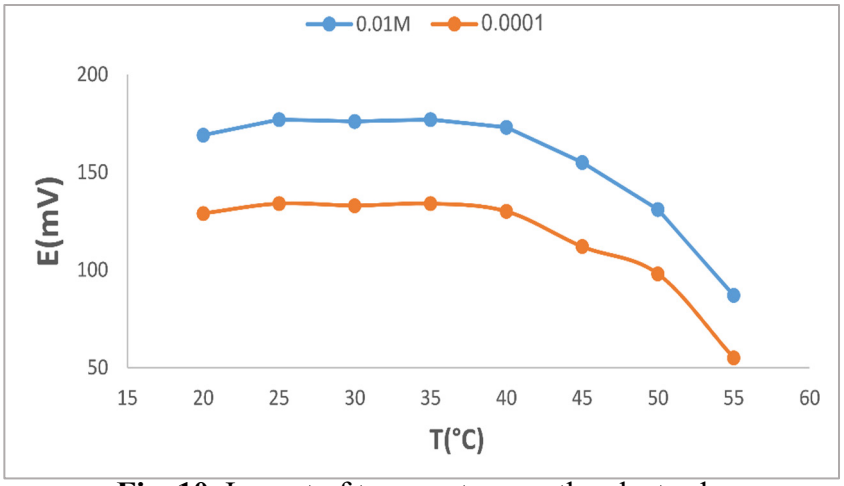

Fig. 10. Impact of temperature on the electrode.

Impact of temperature. According to the data, the electrode's ideal operating temperature is between 20°C and 40°C, as Fig. 10 illustrates. A significant rise in potential was noted above 40°C, which was associated with membrane deterioration. Increased membrane surface area and better PCA drug molecule mobility across the membrane matrix at high temperatures are probably the combined causes of this degradation.

Lifetime of sensor. According to this investigation, the electrode performs steadily for about 23 days. A steady negative drift in potential was seen after this time (Fig. 11). This decrease is

explained by the plasticizer and active component of the membrane gradually leaching from the polymeric matrix.

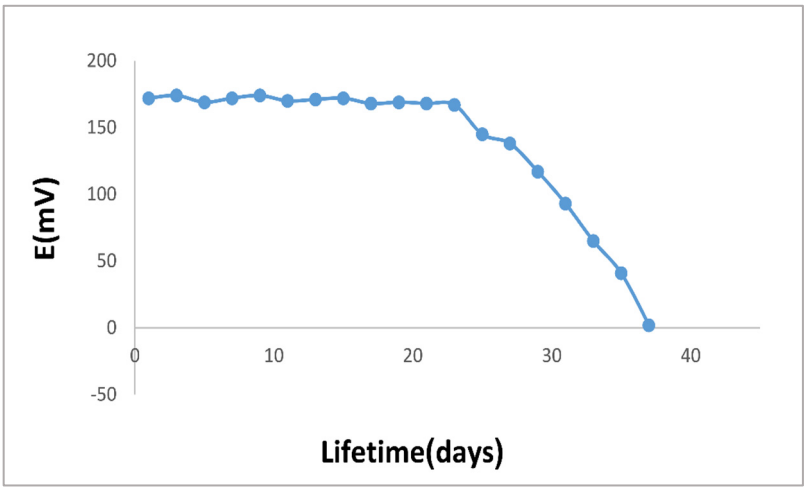

Fig. 11. Lifetime of electrode

Selectivity of PCA electrode. The selectivity coefficient (Kpot A, B) for the nanographite electrode was measured using the separate solution method, according to the following equation [22]: Log Kpot A, B = $(E_B - E_A) / S + (1 - Z_A / Z_B)$ Log a_A.

This equation is known as the Nikolsky-Eisenman equation. The selectivity coefficient depends on the electrode potentials for both the primary (E_A) and interfering (E_B) ions. It also accounts for the charge numbers of these ions (Z_A and Z_B), the activity of the primary ion (a_A), and the slope of the electrode (S). The calculated selectivity coefficients were found to be very small, indicating that the interfering substances have a negligible effect on the electrode's response. The specific values of the selectivity coefficients are listed in Table 3.

Table 3. Selectivity coefficient

Interference ion (0.1 M)	Log $K_{A,B}$	$K^{pot}_{A,B}$
Na^{+1}	- 3.692	1.6×10^{-4}
K^{+1}	- 3.935	1.15×10^{-4}
Mn^{+2}	- 5.784	4.1×10^{-7}
SO_4^{-2}	- 4.410	3.8×10^{-6}
Cl^{-1}	- 4.760	4.3×10^{-5}
NO_2^{-1}	- 4.607	9.8×10^{-5}
Starch	- 5.422	3.9×10^{-5}
Sucrose	- 5.710	1.6×10^{-5}

Calibration plot. Following the optimization of the experimental parameters delineated in Table 4, an assessment of the sensor's potentiometric response was conducted. The constructed working electrode was systematically paired with a standard reference electrode and subsequently immersed in a series of procaine (PCA) standard solutions, with concentrations ranging from 1×10^{-7} M to 1×10^{-2} M. For each concentration level, a consistent electromotive force (emf) reading was meticulously recorded in six independent replicates. The recorded potential values were then correlated with the negative logarithm of the corresponding procaine activity. The resultant calibration graph exhibited a linear relationship throughout the entire concentration range that was evaluated. A quantitative analysis of this plot (Fig. 12) revealed a linear response range extending from 1×10^{-7}M to 1×10^{-2} M, alongside a calibration slope of 22.8 mV per decade. This observed slope exhibits near-Nernstian behavior, showing proximity to the theoretically predicted value of 19.7 mV per decade for a mono-cationic species as derived from the Nernst equation.

Table 4. Method optimum conditions

Variables	value
PMA:PCA volume ratio	1:1
Time response, sec.	7-32
pH range	2-7
Temp., °C	20-40

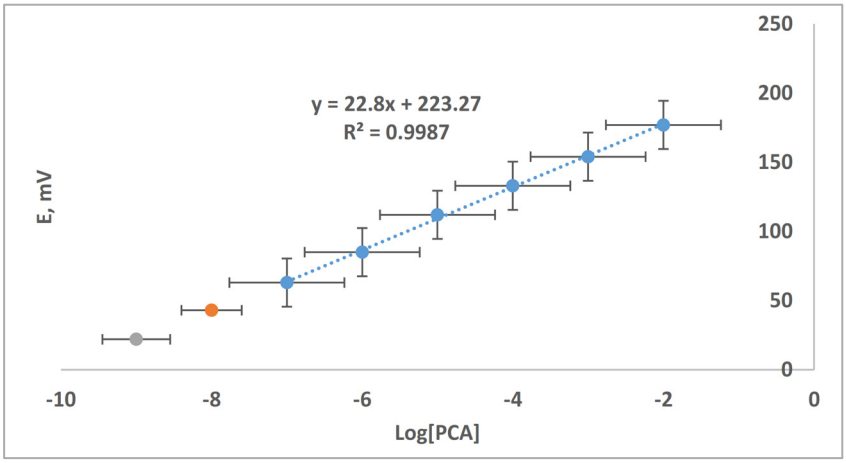

Fig. 12. The calibration plot of PCA using nano graphite electrode

Detection limit. The LOD was calculated by evaluating the minimal conc. of 1×10^{-7} M (six replicates) [23, 24]. The findings are shown in Table 5.

Table 5. Results of LOD

Lowest conc. (C)	*Standard deviation (SD)	*Mean $\overline{X}$ (mv)	LOD (M)
$1x10^{-7}$	3.10	61	1.67×10^{-8}

*Average of six determinations.

Accuracy and precision. By calculating the (RE%), recovery, and RSD% for five different concentrations (1×10-^{2} -1×10^{-7} M), the method's accuracy and precision were confirmed. The (RSD%) and recovery% show how sensitive and precise the procedure is by measuring the potentials for six measurements for each concentration. The results are shown in Table 6.

Table 6. Results of accuracy and precision

Drug Conc. (M)	*Response (mv)	Estimated response (mv)	RE %	Recovery%	RSD%
1×10^{-2}	178	178.651	-0.364	99.636	0.98
1×10^{-3}	156	156.166	-0.106	99.894	1.05
1×10^{-4}	132	132.666	-0.502	99.498	1.12
1×10^{-5}	111	111.663	-0.594	99.406	1.08
1×10^{-6}	85	85.833	-0.97	99.03	1.15
1×10^{-7}	62	63.521	-2.394	97.606	1.20

*Average of six determinations.

Analytical application. The practical analytical utility of the proposed ion-selective electrode (ISE) was validated by determining PCA in its commercial tablet formulation. Using the conventional calibration curve method, the analysis yielded excellent recovery rates of at least 99.72%, with high precision evidenced by a relative standard deviation (RSD) ranging between 0.95% and 1.10% (Table 7).

Table 7. A nano-graphite electrode was used to determine PCA in tablets

Conc. taken (M)	Conc. found (M)	Measured Potential (mv)*	Calculated* Potential (mv)	RE %	Recovery %	RSD %
1×10^{-2}	$1.06X10^{-2}$	177.67	177.3	0.21	100.21	0.95
1×10^{-3}	$9.92X10^{-4}$	154.17	154.6	-0.28	99.72	1.02
1×10^{-4}	$1.13X10^{-4}$	133.13	132	0.86	100.86	1.10
$1\times1\ 0^{-5}$	$1.1X10^{-5}$	112.33	112.7	-0.33	99.6	1.08

**Average of six determinations.*

Conclusion

This study successfully demonstrated a green and sustainable synthesis method for crystalline strontium nanoparticles using a natural thyme extract. The synthesized nanoparticles, characterized by their small crystallite size and high surface area, were integral to the performance of a new potentiometric procaine sensor. The fabricated sensor exhibited excellent analytical properties, including a wide linear range, a low detection limit, high selectivity, and a stable operational lifetime. The successful application of the sensor in determining procaine in pharmaceutical tablets confirms its practical utility and establishes its potential for use in industrial quality control. This work not only contributes a new, high-performance analytical tool to the field of pharmaceutical analysis but also presents a strong case for the continued exploration of green chemistry in the development of advanced functional nanomaterials.

References

1. Brunton L.L., Hilal-Dandan R., Knollmann B.C. *Local Anesthetics. In: Goodman & Gilman's: The Pharmacological Basis of Therapeutics*. 14th ed. New York. McGraw-Hill Education. 2023.
2. Katzung B.G. *Local Anesthetics. In: Basic & Clinical Pharmacology*. 15th ed. New York. McGraw-Hill Education. 2021.
3. Moffat A.C., Osselton M.D., Widdop B., Watts J. *Clarke's Analysis of Drugs and Poisons*, 4th ed. London: Pharmaceutical Press. 2011.
4. *British Pharmacopoeia Commission. Procaine Hydrochloride*. In: British Pharmacopoeia, London: The Stationery Office. 2022.
5. Berkel C., Özbek O. Green electrochemical sensors, their applications and greenness metrics used: a review. *Electroanalysis*, 2024, **Vol. 36(11)**, e202400286. DOI: 10.1002/elan.202400286
6. Isildak Ö., Özbek O. Application of potentiometric sensors in real samples. *Critical Reviews in Analytical Chemistry*, 2021, **Vol. 51(3)**, p. 218-231. DOI: 10.1080/10408347.2019.1711013
7. Shawish H.M., Ghalwa N.A., Al-Kashef I.D., Saadeh S.M., Almonem K.I. Extraordinary enhancement of a 5-fluorouracil electrode by praepagen HY micellar solutions. *Microchemical Journal*, 2020, **Vol. 152**, 104316. DOI: 10.1016/j.microc.2019.104316
8. Özbek O., Ugur Ö.B., Ören S., Gürdere M.B., Kocabas S. New solid state contact potentiometric sensor based on a thiosemicarbazone derivative molecule for determination of copper (II) ions in environmental samples. *Polyhedron*, 2024, **Vol. 252**, 116878. DOI: 10.1016/j.poly.2024.116878
9. Wu Y., Qileng A., Bakker E. Self-powered optical ion sensor array based on potentiometric probes coupled to electronic paper. *Sensors and Actuators B: Chemical*, 2023, **Vol. 396**, 134561. DOI: 10.1016/j.snb.2023.134561
10. Verma S., Sharma A.K., Shukla S.K. Self-fuelled nickel oxide encapsulated sodium alginate-grafted-polypyrrole for potentiometric sensing of lead ions. *Materials Science and Engineering: B*, 2023, **Vol. 293**, 116469. DOI: 10.1016/j.mseb.2023.116469
11. Özbek O., Isildak Ö. Potentiometric PVC membrane sensor for the determination of anti-epileptic drug levetiracetam in pharmaceutical formulations. *ChemistrySelect*, 2022, **Vol. 7(3)**, e202103988. DOI:10.1002/slct.202103988

12. Özbek O., Altunoluk O.C. Potentiometric determination of the local anesthetic procaine in pharmaceutical samples. *Analytical Biochemistry*, 2024, **Vol. 695**, 115657. DOI: 10.1016/j.ab.2024.115657
13. Özbek O., Çetin A., Koc E., Isildak Ö. Synthesis and sensor properties of a phenol derivative molecule: potentiometric determination of silver (I) ions. *Electrocatalysis*, 2022, **Vol. 13(4)**, p. 486-493. DOI: 10.1007/s12678-022-00738-2
14. Singh J., Dutta T., Kim K.H., Rawat M., Samddar P., Kumar P. 'Green' synthesis of metals and their oxide nanoparticles: applications for environmental remediation. *Journal of Nanobiotechnology*, 2018, **Vol. 16(1)**, p. 84. DOI: 10.1186/s12951-018-0408-4
15. Zulfugarova S.M., Azimova G.R., Aleskerova Z.F. Synthesis of cobalt and copper nanoferrites by a sol-gel method using plants and their catalytic activity. *Chemical Problems*, 2026, **Vol. 24(3)**, p. 465-475. DOI: 10.65382/2221-8688-2026-3-465-475
16. İmamaliyeva A.A., Chiraqov F.M., Hajiyeva F.V., Quliyeva F., Musayeva N.N. Synthesis and structural characterization of new complexes based on silver nanoparticles, dithiooxamide reagent, and cetyltrimethylammonium bromide. *Chemical Problems*, 2026, **Vol. 24(1)**, p. 138-146. DOI: 10.65382/2221-8688-2026-1-138-146
17. Paul S., Chakraborty B.B., Deb K., Choudhury S. Fused ring heterocycle functionalized gold nanoparticles: synthesis and self-assembly. *Chemical Problems*, 2023, **Vol. 21(2)**, p. 188-196. DOI: 10.32737/2221-8688-2023-2-188-196
18. Iravani S. Green synthesis of metal nanoparticles using plants. *Green Chemistry*, 2011, **Vol. 13(10)**, p. 2638–2650. DOI: 10.1039/C1GC15386B
19. Jha A.K., Prasad K. Green Synthesis of Strontium Nanoparticles and Their Applications in Medicine and Catalysis. *In: Micro and Nano Technologies*, 2016, p. 105-122.
20. Mittal A.K., Chisti Y., Banerjee U.C. Synthesis of metallic nanoparticles using plant extracts. *Biotechnology Advances*, 2013, **Vol. 31(2)**, p. 346-356. DOI:10.1016/j.biotechadv.2013.01.003
21. Borase H.P., Patil C.D., Salunkhe R.B., Suryawanshi R.K., Salunke B.K., Patil S.V. Phytolatex synthesized silver nanoparticles: a new approach towards mosquito control. *Asian Pacific Journal of Tropical Disease*, 2014, **Vol. 4(Suppl 1)**, p. S204-S210. DOI: 10.1111/ics.12158
22. Maj-Zurawska M., Lewenstam A. Selectivity coefficients of ion-selective magnesium electrodes used for simultaneous determination of magnesium and calcium ions. *Talanta*, 2011, **Vol. 87**, p. 295-301. DOI: 10.1016/j.talanta.2011.09.023
23. Atiyah A.M., Hussein K.S., Ahmed A.M. Fabrication of ion selective pvc membrane sensor for potentiometric determination of escitalopram oxalate in its pure form and pharmaceutical tablet. *Bulletin of Pharmaceutical Sciences Assiut University*, 2024, **Vol. 47(1)**, p. 261-272. DOI: 10.21608/bfsa.2024.277943.2064
24. Ahmed A.M., Hanoon I.T., Ahmed S.H. Determination of the ciprofloxacin hydrochloride drug in some pharmaceuticals using manufactured membrane selective electrodes. *Systematic Reviews in Pharmacy*, 2020, **Vol. 11**, p. 622-626. DOI: 10.31838/srp.2020.6.92